

A physical model of the turbulent boundary layer consonant with mean momentum balance structure

BY JOE KLEWICKI^{1,*}, PAUL FIFE², TIE WEI³ AND PAT MCMURTRY⁴

¹*Department of Mechanical Engineering, University of New Hampshire, Durham, NH 03824, USA*

²*Department of Mathematics, and* ⁴*Department of Mechanical Engineering, University of Utah, Salt Lake City, UT 84112, USA*

³*Department of Mechanical and Nuclear Engineering, Pennsylvania State University, State College, PA 16802, USA*

Recent studies by the present authors have empirically and analytically explored the properties and scaling behaviours of the Reynolds averaged momentum equation as applied to wall-bounded flows. The results from these efforts have yielded new perspectives regarding mean flow structure and dynamics, and thus provide a context for describing flow physics. A physical model of the turbulent boundary layer is constructed such that it is consonant with the dynamical structure of the mean momentum balance, while embracing independent experimental results relating, for example, to the statistical properties of the vorticity field and the coherent motions known to exist. For comparison, the prevalent, well-established, physical model of the boundary layer is briefly reviewed. The differences and similarities between the present and the established models are clarified and their implications discussed.

Keywords: wall-turbulence; scaling; flow physics; mean momentum balance

1. Introduction

Fluid dynamic boundary layers form in flows tangential to a no-slip wall. A foundational notion pertaining to the boundary layer is that there is *always* a region near a no-slip surface within which the direct effects of viscosity are dynamically significant (Prandtl 1904; Schlichting 1979). With increasing Reynolds number, this region necessarily becomes a decreasing fraction of the overall flow domain. In this manner, the solution to the Navier–Stokes equation approaches that of the Euler equation as the Reynolds number becomes large (e.g. a limiting model for the boundary layer is a vortex sheet positioned infinitesimally above the wall). Given this, a central objective of boundary layer theory is to determine this rate at which the effects of viscosity become spatially localized.

* Author for correspondence (joe.klewicki@unh.edu).

One contribution of 14 to a Theme Issue ‘Scaling and structure in high Reynolds number wall-bounded flows’.

In connection to dynamics, attaining this objective also serves to reveal the scaling behaviour of the momentum field, since doing so effectively determines the normalization required to write the momentum balance equation in a form that remains invariant for varying Reynolds number. Perhaps, the most famous example of this pertains to the flat plate laminar boundary layer, as the well-established $1/\sqrt{R_x}$ scaling behaviour directly reflects the rate at which viscous effects diminish (spatially localize) with increasing Reynolds number. As might be expected, identifying the dominant terms in the momentum balance along with those normalizations that retain this balance independent of Reynolds number (i.e. the Reynolds number scalings) also provides a basis for educing flow physics. For example, the $1/\sqrt{R_x}$ behaviour is also directly associated with the dynamics realized via the competition between the advection and the wall-normal diffusion of axial momentum.

Of course, determining the scaling behaviours associated with the mean momentum field development in smooth-wall turbulent boundary layers is considerably more challenging. Primary reasons for this are that (i) the mean momentum equation is indeterminate owing to the appearance of the Reynolds stresses and (ii) in some turbulent wall-flows, there are subregions within which viscous effects are negligible in the mean. These challenges notwithstanding, significant progress has recently been made towards identifying the appropriate approximate forms of the mean momentum balance (MMB) as the layer is traversed, as well as in identifying those normalizations that render these simplified forms of the equation invariant with variations in Reynolds number (Fife *et al.* 2005*a,b*; Wei *et al.* 2005*a*).

The primary purposes of the current effort are to present a physical model of the turbulent boundary layer that is consistent with the structure of the MMB and to compare it with the established prevalent model.

2. The prevalent physical model

For the purpose of comparison, this section provides a relatively brief discussion of the predominant, well-accepted, model of the turbulent boundary layer.

(a) Mean profile-based layer structure and scaling behaviours

The prevalent physical model of the mean structure of the smooth-wall turbulent boundary layer has rather direct connection to the properties of the mean velocity profile (e.g. Tennekes & Lumley 1972; Pope 2000; Davidson 2004). (Herein, x is the axial coordinate, y is the wall normal coordinate, U and V are the velocity components in the x - and y -directions, respectively, upper case letters represent mean quantities, lower case letters denote fluctuating quantities, tilde denotes instantaneous quantities (i.e. $\tilde{u} = U + u$), an overbar denotes time averaging and vorticity components are identified by their subscript.) Figure 1*a* shows representative turbulent boundary-layer mean velocity profiles. These profiles have been made non-dimensional using inner variables, u_τ and ν , where $u_\tau = \sqrt{\tau_w/\rho}$ is the friction velocity, τ_w is the wall shear stress and ν is the kinematic viscosity, as denoted by a superscript ‘+’. Thus, a Reynolds number based on the friction velocity and the boundary layer thickness, δ , is given by $\delta^+ = \delta u_\tau/\nu$. As is conventional, the data in figure 1 are

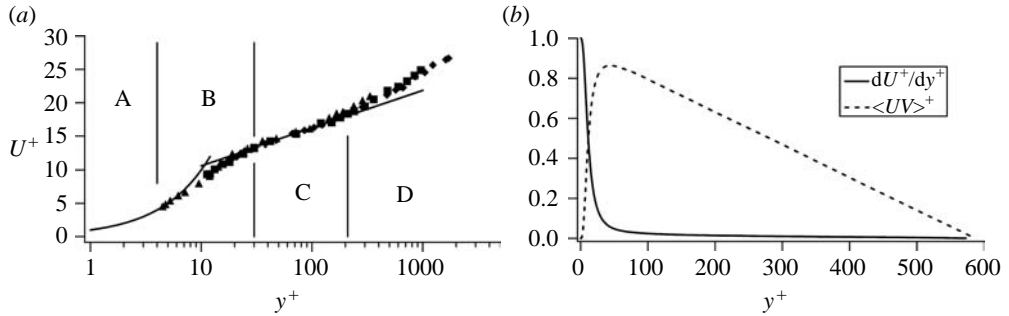


Figure 1. Inner-normalized mean velocity and stress profiles. (a) Turbulent boundary layer mean profiles and their associated layer structure: (A) viscous sublayer, (B) buffer layer, (C) logarithmic layer and (D) wake layer (data are from Klewicki & Falco (1990)). (b) Viscous and Reynolds shear stress profiles in turbulent channel flow, $\delta^+ = 590$, where in this case δ is the half channel height. These data are from Moser *et al.* (1999).

plotted on semi-logarithmic axes. The main features of this graph are (i) a layer immediately adjacent to the surface where the normalized profile is linear (A), (ii) a layer where the dependence of U^+ on y^+ transitions from linear to approximately logarithmic (B),¹ (iii) a region of approximately logarithmic variation (C), followed by (iv) an extensive outer region within which U^+ varies according to a function consisting of a logarithmic part plus a wake part, $w(y/\delta)$. Dynamically, the viscous sublayer (A), $0 \leq y^+ \leq 4$, is identified as a region where viscosity has a major effect. In the buffer layer (B), $4 \leq y^+ \leq 30$, the viscous and Reynolds stresses are both dynamically significant. The logarithmic layer (C) extends from near $y^+ = 30$ to $y/\delta \approx 0.2$ and is seen to be dominated by the effects of turbulent inertia. Within the wake layer (D), $0.2 \leq y/\delta \leq 1$, mean and turbulent inertia are predominant.

Attaching these time-averaged dynamical attributes to layers A–D is typically justified by examining the relative magnitudes of the mean viscous stress, $\partial U^+/\partial y^+$, and the Reynolds shear stress, $T^+(y^+) = -\overline{wv}^+$ (e.g. Tennekes & Lumley 1972; Pope 2000; Davidson 2004). Representative profiles of these quantities are shown in figure 1b. These data reveal that the magnitude of T^+ is zero at the wall, but rapidly rises to a value that is $O(1)$ by $y^+ \approx 30$. Conversely, $\partial U^+/\partial y^+ = 1.0$ at $y^+ = 0$, but diminishes to a quantity that is much less than $O(1)$ by $y^+ \approx 30$. (Herein, the order symbol, $O(\cdot)$, will be used with respect to $\epsilon \rightarrow 0$, where ϵ is a small parameter, e.g. $\epsilon^2 = 1/\delta^+$. For example, $a = O(b)$ for positive $a(\epsilon)$ and $b(\epsilon)$ is taken to mean that both a/b and b/a are bounded as $\epsilon \rightarrow 0$.) These observations are commonly used to support the notion that, in the mean, the dynamical effects of inertia become greater than those of viscosity beginning in layer B and predominantly so with the outward distance from layer B.

Examination of the layer thicknesses and the velocity increments across these layers reveals the Reynolds number dependencies inherent to this physical model. These dependencies are listed in table 1. As is apparent from the entries

¹Note that approximately logarithmic does not exclude certain power-law forms. Also, recent experimental data provide evidence that the traditionally defined *logarithmic* layer is composed of two regions having logarithmic-like behaviour, but not necessarily the same slope (Osterlund *et al.* 2000; McKeon *et al.* 2004).

Table 1. Scaling behaviours of the layer thicknesses and layer velocity increments associated with the predominantly accepted physical layer structure of the turbulent boundary layer (C , D and E are constants).

physical layer	Δy increment	ΔU increment
A (viscous sublayer)	$O(v/u_\tau)$ ($\simeq 4$)	$O(u_\tau)$ ($\simeq 4$)
B (buffer layer)	$O(v/u_\tau)$ ($\simeq 26$)	$O(u_\tau)$ ($\simeq 9$)
C (logarithmic layer)	$O(\delta)$ ($\rightarrow 0.2\delta$)	$O(U_\infty)$ ($\simeq (u_\tau/\kappa)\log(\delta/C)$)
D (wake layer)	$O(\delta)$ ($\simeq 0.8\delta$)	$O(U_\infty)$ ($\simeq (u_\tau/\kappa)\log(\delta/D)+E$)

in table 1, the layers associated with the direct effects of viscosity (A and B) have a thickness that remains a fixed number of viscous lengths independent of Reynolds number. Correspondingly, with increasing δ^+ , these layer thicknesses become a diminishingly small fraction of δ at a rate directly proportional to $1/\delta^+$. Similarly, the velocity increments across these layers are measured by a fixed number of u_τ , and thus as $\delta^+ \rightarrow \infty$, they become diminishingly small relative to U_∞ at a rate proportional to u_τ/U_∞ . Conversely, both the logarithmic layer and the wake layer grow at a rate proportional to δ as $\delta^+ \rightarrow \infty$. Of course, when measured in viscous lengths, these layer thicknesses are unbounded as $\delta^+ \rightarrow \infty$. In a similar manner, the velocity increment across either layer C or D approaches a fixed fraction of U_∞ as $\delta^+ \rightarrow \infty$.

(b) Dynamical considerations

Important elements associated with the predominant model relate to the derivation of the logarithmic mean velocity profile. While other derivations exist, the construction commonly deemed most rigorous postulates the existence of a two-layer mathematical structure (*inner* and *outer*), and *assumes* that the inner and outer scalings have a common region of *overlap* within which both are simultaneously valid (e.g. Millikan 1939; Tennekes & Lumley 1972; Pope 2000; Panton 2005). Under further assumption that the profile strictly increases with y , the mean velocity gradient (simultaneously expressed in its inner and outer forms) is matched in the overlap layer as $y^+ \rightarrow \infty$ and $\eta \rightarrow 0$. The classical forms of the logarithmic *law of the wall* and *defect law* subsequently follow. According to this description, the inner layer extends from the wall to the outer edge of the logarithmic layer, and the outer layer extends from the inner edge of the logarithmic layer to δ . An important physical implication of this mathematical description is the correspondence between the overlap layer and an inertial sublayer. Thus, considerable research has been devoted towards understanding logarithmic layer turbulence and its similarities to the spectral version of inertial range turbulence (e.g. Townsend 1976; Perry & Abell 1977; Perry & Marusic 1995; Morrison *et al.* 2004; Davidson *et al.* 2006; McKeon & Morrison 2007; Metzger 2006).

Other considerations pertain to how any given model sets the conceptual framework for interpreting measurements and observations. Notable among these relate to describing the characteristics and dynamical behaviours of boundary-layer coherent motions. A comprehensive review of boundary-layer coherent motions is well beyond the scope of the present effort. It is useful however to identify

the implications of the predominant model relative to the interpretation of dynamical processes. To this end, issues relating to the self-sustaining mechanisms and the so-called inner/outer interaction are now briefly discussed.

As supported by the stress profiles of figure 1*b* and other near-wall statistical data (e.g. the turbulence kinetic energy profile), the prevalent model places high importance on the near-wall region (buffer layer and below; e.g. Robinson 1990). Numerous coherent motions have been identified as dynamically significant in this region—including streaks, pockets, streamwise vortices, internal shear layers and hairpin vortices. Indeed, this region is asserted by many to be where the self-sustaining mechanisms of boundary layer turbulence primarily reside (e.g. see a number of contributions to Panton 1997). It is also generally accurate to attribute this focus on the near-wall region with the identification of the buffer layer as where the dynamics transition from being strongly influenced by viscosity to where turbulent inertia dominates (Pope 2000; Davidson 2004).

This last notion also has bearing on how to construct a description of the so-called inner/outer interaction. Properly characterizing the nature of the interactions between the inner and the outer layers is asserted by many to be central to understanding turbulent boundary layer dynamics (e.g. Kline 1978; Falco 1983; Thomas & Bull 1983; Klewicki 1989; Sreenivasan 1989; Wark & Nagib 1991). This assertion finds support from at least two compelling arguments. At perhaps the most fundamental level, the turbulent boundary layer may be considered a fluid dynamical machine that, on an average, converts free-stream momentum into tangential force acting at the fluid/solid interface. Given this, one is then faced with describing how the net momentum transfer across the layer occurs, and thus the inner/outer interaction. Similarly, a primary characteristic of the boundary layer is that with increasing δ^+ the ratio of the outer to the inner length-scale increases. The inner/outer interaction is unavoidably confronted if the dynamical accommodation to this scale separation is to be described. Apparently, owing to its inherent complexities, the inner/outer interaction remains resistive to a thorough characterization. For example, if the viscous/inertial interaction is seen as central to the inner/outer interaction, then the prevalent model places it in the buffer layer for all δ^+ . On the other hand, by definition, the overlap region is where inner and outer scalings are simultaneously valid, and thus justification to primarily associate inner/outer interactions with the logarithmic layer. Doing so, however, requires explaining why inner/outer interactions should occur in an inertial sublayer,² and not in the region where the viscous and Reynolds stresses are of the same order of magnitude.

Lastly, a significant and growing body of results (Wark & Nagib 1991; Meinhart & Adrian 1995; Adrian *et al.* 2000; Ganapathisubramani *et al.* 2003, 2005; Tomkins & Adrian 2003; Morris *et al.* in press; Priyadarshana *et al.* 2007) support the perspective that the logarithmic layer is instantaneously composed of a hierarchy of motions, and that these motions are nominally arranged as uniform momentum zones segregated by relatively narrow vortical fissures. At present, it is not readily apparent how such an instantaneous structure might give rise to a mathematical description based upon an overlap layer. This type of

²Empirical observations relating to the behaviour of the logarithmic mean profile have recently prompted proposals regarding the existence of a meso-layer (Wosnik *et al.* 2000) in the region $30 \leq y^+ \leq 300$ and an extended ‘buffer region’ (Osterlund *et al.* 2000) out to about $y^+ = 200$.

hierarchical structure however would seem to have a rather natural connection to the earlier, phenomenological, log profile derivation based upon postulating the distance from the wall as the appropriate length-scale (Prandtl 1925).

3. An alternative physical model

Recent empirical observations and multiscale analysis provide the basis for an alternative physical model of the turbulent boundary layer (Fife et al. 2005a,b; Wei et al. 2005a,b). An important premise underlying the layer structure to be described, and in turn the alternative physical model, is that the MMB in its unintegrated form (and in this case as applied to boundary layer flow over a planar surface located at $y=0$),

$$U^+ \frac{\partial U^+}{\partial x^+} + V^+ \frac{\partial U^+}{\partial y^+} = \frac{\partial^2 U^+}{\partial y^{+2}} + \frac{\partial T^+}{\partial y^+}, \quad (3.1)$$

provides the time-averaged description of the dynamics. The left side of equation (3.1) represents advection by the mean flow, while the right-side terms represent the viscous and Reynolds stress gradients, respectively. For the flat plate flow, there are only these three distinct dynamical effects, and thus the ratio of any two determines the nature by which the equation is balanced.

(a) MMB-based layer structure and scaling behaviours

Wei et al. (2005a) explored the structure of boundary layer, pipe and channel flows by examining the ratio of the last two terms in equation (3.1). The dynamics reflected by equation (3.1) must arise from a balance of at least two non-negligible terms, and thus interpretation of this ratio is as follows.

- (i) If $|(\partial^2 U^+/\partial y^{+2})/(\partial T^+/\partial y^+)| \gg 1$, then the Reynolds stress gradient term is negligible and equation (3.1) sums to zero essentially through a balance of the mean advection and viscous stress gradient terms.
- (ii) If $|(\partial^2 U^+/\partial y^{+2})/(\partial T^+/\partial y^+)| \ll 1$, then the mean viscous stress gradient term is negligible and equation (3.1) sums to zero essentially through a balance of the mean advection and Reynolds stress gradient terms.
- (iii) If $|(\partial^2 U^+/\partial y^{+2})/(\partial T^+/\partial y^+)| \approx 1$, then the Reynolds stress and the viscous stress gradients balance and are either greater than or of the same order of magnitude as the mean advection term.

Available high-quality experimental and DNS data (Zagarola & Smits 1997; Moser et al. 1999; DeGraaff & Eaton 2000) were differentiated and the indicated ratio was examined as a function of y for differing δ^+ . The sketch of figure 2 depicts the behaviour of the stress gradient ratio at any fixed δ^+ . As indicated, the dynamical balance is described by a four-layer structure. Layer I essentially retains the character of the viscous sublayer, and in the boundary layer is a region where the viscous stress gradient nominally balances mean advection. In layer II, the magnitude of the ratio is very close to unity, and thus this layer is called the stress gradient balance layer. Across the mesolayer (layer III), the Reynolds stress gradient changes sign and the terms in equation (3.1) undergo a *balance breaking and exchange* (Fife et al. 2005b; Wei et al. 2005a). Within layer III, all the three

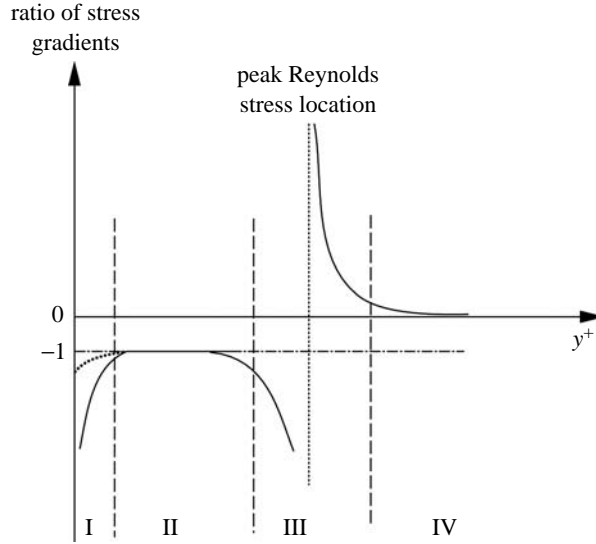


Figure 2. Sketch of the ratio of the viscous stress gradient to the Reynolds stress gradient in boundary layer, pipe and channel flows at any given Reynolds number. The dotted line in layer I is for a boundary layer, and the solid line is for a pipe or channel.

Table 2. Scaling behaviours of the layer thicknesses and velocity increments of the proposed alternative model. (Note that the layer IV properties are asymptotically attained as $\delta^+ \rightarrow \infty$.)

physical layer	Δy increment	ΔU increment
I	$O(v/u_\tau)$ (≈ 3)	$O(u_\tau)$ (≈ 3)
II	$O(\sqrt{v\delta}/u_\tau)$ (≈ 1.6)	$O(U_\infty)$ ($\approx U_\infty/2$)
III	$O(\sqrt{v\delta}/u_\tau)$ (≈ 1.0)	$O(u_\tau)$ (≈ 1)
IV	$O(\delta)$ ($\rightarrow \delta$)	$O(U_\infty)$ ($\rightarrow U_\infty/2$)

terms in equation (3.1) are nominally of the same order of magnitude,³ and from the outer edge of layer III to $y = \delta$ (i.e. layer IV), equation (3.1) is characterized by a balance between the mean advection and the Reynolds stress gradient.

The features of figure 2, depicted for fixed δ^+ , persist for the δ^+ range currently accessible to inquiry (e.g. spatial resolution in the Princeton Superpipe limited the Reynolds number to $R^+ \leq 41\,235$). In this regard, it is also relevant to note that boundary layer and pipe/channel flows exhibit the same behaviours to within the differences between the mean advection and pressure gradient profiles. Thus, for example, in layer II their structure is expected to be highly similar since in this layer these terms are much smaller than the dominant stress gradient terms. Quantitatively, the layer thicknesses and the velocity increments across these layers have been shown both empirically and analytically to exhibit distinct Reynolds number dependencies. Table 2 presents these scaling

³Of course, right at the peak in the Reynolds stress the Reynolds stress gradient passes through zero, and thus in a narrow zone around this point within layer III the Reynolds stress gradient is smaller than the other two terms.

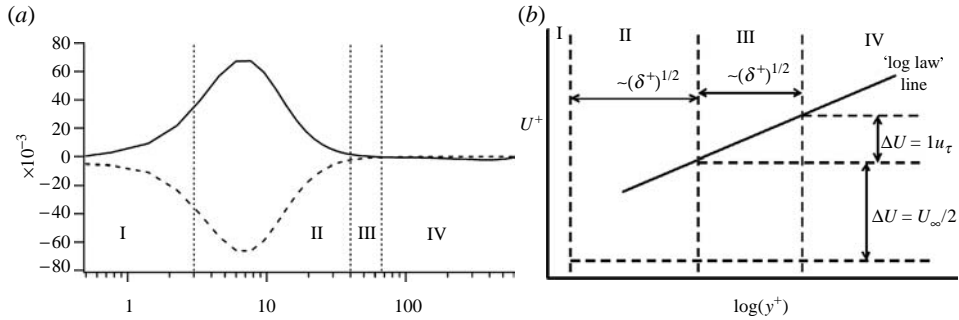


Figure 3. Attributes of layers II and III: (a) inner normalized Reynolds stress gradient (solid line) and viscous stress gradient (dashed line) profiles (data are from the $R_\theta=1410$ DNS of Spalart (1988)) and (b) schematic depiction of the connection between the growth rates of layers II and III and their associated velocity increments.

behaviours. As is evident, layers I and IV adhere to inner and outer scaling, respectively. On the other hand, layers II and III exhibit mixed scaling properties. The inner normalized thickness of layer II grows like the geometric mean of the Reynolds number (i.e. $\sim\sqrt{\delta^+}$), while its velocity increment remains a fixed fraction of U_∞ , independent of δ^+ . Similarly, $\Delta_{III}y^+ \sim\sqrt{\delta^+}$, while its velocity increment is only about $1.0u_\tau$, independent of δ^+ . These scaling behaviours differ considerably from the prevalent model and are associated with the existence of a third fundamental length-scale, $\sqrt{\nu\delta/u_\tau}$. This length is intermediate to ν/u_τ and δ , required to scale the MMB in layer III and becomes increasingly distinct as $\delta^+ \rightarrow \infty$.

The mean dynamics and scaling behaviours associated with layers II and III are central (and apparently unique) to the proposed physical model, and thus warrant further discussion. Layer II is called the stress gradient balance layer since the dominant dynamical mechanisms are the terms on the right of equation (3.1); their ratio being -1 in figure 2. Contrary to the prevalent notion that, on an average, boundary layer dynamics are dominated by turbulent inertia outside the buffer layer (independent of δ^+), momentum balance data reveal that an equal competition between the viscous force and the turbulent force persists to a y -location near the peak in the Reynolds stress, T_{\max} . Consistent with the mathematical hierarchy of scaling layers revealed by Fife *et al.* (2005a), in the model posed below this competition is associated (in a time-mean sense) with the vortical motions forming and evolving from the near-wall vorticity field. It is significant to note, however, that the balance in layer II comes about via two opposite sign, nearly equal, but decreasing magnitude functions. These functions lose dominance over mean advection as layer II transitions into layer III (figure 3a).

The scalings of table 2 reveal that the layer II and III thicknesses are coupled, such that their velocity increments follow outer and inner scaling, respectively. These properties underlie new interpretations relating to, for example, the nature of the inner/outer interaction in boundary layers. It is relevant to note that the major portions of layers II and IV and all of layer III reside within the bounds of the traditionally defined logarithmic layer. The lower edge of layer II is fixed near the edge of the viscous sublayer (independent of δ^+), while the position of its

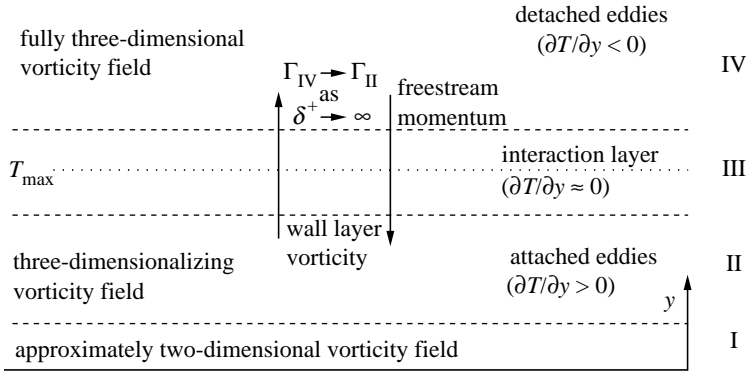


Figure 4. Schematic of some of the dynamical attributes of the proposed model for the turbulent boundary layer. Layer numbers are the same as those identified in figure 2. Note that the position of T_{\max} , y_{\max}^+ , varies like $\sqrt{\delta^+}$.

outer edge extends to increasing y^+ values like $\sqrt{\delta^+}$, such that $\Delta_{II} U = U_{\infty} / 2$. (Note that under outer normalization the position of the outer edge of layer II moves ‘inward’ like $1 / \sqrt{\delta^+}$.) Owing to this positioning behaviour for layer II, both the end points of layer III vary with δ^+ , particularly, like $\sqrt{\delta^+}$. Thus, while the layer III thickness exhibits the same Reynolds number scaling behaviour as layer II, its velocity increment is only $\approx 1 u_{\tau}$. This arises owing to the fact that with increasing δ^+ , layer III is positioned at increasing y^+ -locations in a region where $U^+ \approx \log(y^+)$ (figure 3b).

(b) Physical interpretation

Elements of a new physical model are represented in the schematic of figure 4. Unlike the physical picture promoted by the prevalent view, this model is specifically constructed to be consistent with the MMB properties. This leads to a number of new interpretations relating to the description of flow physics. Of course, it is recognized that any defensible physical model should also embrace the numerous independent empirical observations relating, for example, to the boundary-layer coherent motions discussed previously. Existing experimental observations are now interpreted in the context of this new model.

(c) Characteristic vortical motions

Since $\tilde{\omega} \neq 0$ provides perhaps the most useful criterion for distinguishing the boundary layer from the free-stream, the process of describing the proposed model begins by attributing the characteristic vortical motions to layers I–IV. Since the properties of layer III are largely attributed to the interaction between layers II and IV, the discussion proceeds according to a I, II, IV, III order.

(i) Layer I

Existing physical and numerical experiments reveal that the vorticity field in the region $0 \leq y^+ \leq 3$ has a perturbed sheet-like character that predominantly meanders in the x - and z -plane, but has little wall-normal component (e.g. Kim *et al.* 1987; Balint *et al.* 1991; Klewicki 1997). Positive $\tilde{\omega}_z$ (i.e. opposite sign to

the mean vorticity) is virtually non-existent in this region (Klewicki *et al.* 1990; Rajagopalan & Antonia 1993; Metzger & Klewicki 2001). Perturbations of this sheet-like distribution of vorticity are believed by many to constitute the initial conditions that trigger the evolution of motions arising out of layer I (Offen & Kline 1974; Perry & Chong 1982; Wallace 1982; Smith *et al.* 1991).

(ii) *Layer II*

At the lower edge of layer II, the vorticity field is highly aligned in the spanwise direction. Across this layer, the vorticity field three dimensionalizes. The associated characteristics are a rapid reduction in $|\Omega_z|$, the appearance of positive $\tilde{\omega}_z$ and a trend towards $\omega'_x = \omega'_y = \omega'_z$, where superscript ‘’ denotes r.m.s. (e.g. Klewicki *et al.* 1990; Balint *et al.* 1991). As indicated in figure 4, this layer is primarily associated with the attached eddies; attached in the sense that their etiology is attributable to the three dimensionalization of the near-wall vorticity field. Note that for all of the descriptions given, the eddies and the dynamics attributed to any given layer should be viewed as probabilistic with a changing mixture of characteristic properties in traversing from one layer to the next. Thus, attached eddies are viewed as predominantly populating layer II, and to a decreasing degree with increasing y^+ across layer III and into layer IV. A significant body of research supports the hypothesis that hairpin-like vortices constitute a basic building block of wall turbulence (e.g. Theodorsen 1952; Head & Bandyopadhyay 1981; Wallace 1982; Perry *et al.* 1986; Smith *et al.* 1991; Adrian *et al.* 2000; Ganapathisubramani *et al.* 2005). Broadly speaking, hairpin vortices are seen to form via the redistribution of near-wall vorticity (mainly composed of $\tilde{\omega}_z$), and subsequently evolve outward. While earlier flow visualization-based evidence indicated that these motions might extend from the sublayer to the edge of the boundary layer (Head & Bandyopadhyay 1981), an increasing and predominantly more recent body of results indicate that at some y -position the vortical motions lose connection with their near-wall origin. Consistent with these studies, the primary candidate eddies for layer II are hairpin-like vortices that collectively organize into hierarchical packets. In this regard, the evolution of the vorticity in these motions is generally attributed to a competition between vortex stretching and viscous diffusion.

(iii) *Layer IV*

Properties of the vorticity field in layer IV include essentially equal vorticity component intensities and a negligible mean vorticity. The vorticity probability distributions however are relatively long tailed—reflecting the increasingly intermittent nature of the vorticity fluctuations (e.g. Balint *et al.* 1991). Given these characteristics, the vortical motions associated with layer IV are identified as detached eddies; detached in the sense that these spatially compact motions are uncorrelated with the near-wall vorticity field, and nominally advect with the layer IV mean flow. Though a specific geometric form for the detached eddies is not completely established, direct measurements of near-wall $\tilde{\omega}_z$ structure, the increasingly three-dimensional nature of the vorticity field with increasing distance from the surface and data considerations relative to $\nabla \cdot \tilde{\omega} = 0$ (Klewicki *et al.* 1990; Rajagopalan & Antonia 1993) support the expectation that at some y -position the characteristic vortical motions become spatially localized and

topologically form closed loops. Detached eddies are hypothesized to predominantly populate layer IV, and to a decreasing degree with decreasing y^+ across layer III and into layer II. The simplest form of such an eddy is a vortex ring-like motion. Falco's earlier 'typical eddy' observations (Falco 1977, 1983, 1991) support the existence of intermediate scale ring-like eddies in both the inner and outer regions. Regardless of the exact geometric form of the detached eddies, a hypothesized characteristic feature is that they contain positive $\bar{\omega}_z$, known to be prevalent in layer IV.

(iv) Layer III

Given the attributes of layers II and IV, layer III is viewed as a zone within which the characteristic eddy transitions from attached to detached with increasing y . Thus, within layer III the expectation is to find a nearly equal mixture of attached and detached eddies. Similarly, the process by which attached eddies might evolve into detached eddies is expected to be characteristic of layer III. In this regard, the recent simulations of Bake *et al.* (2002) provide compelling evidence for the formation of vortex rings from the pinch-off of the legs of hairpin-like vortices during the latest stages of transition. This process was previously proposed by Falco as a mechanism for ring-like motion formation in the turbulent boundary layer, and was explored numerically by Moin *et al.* (1986). The attached-detached eddy decomposition of the vorticity field finds support from visual studies (Falco 1983, 1991; Klewicki 1997), two-point vorticity correlations (Klewicki & Falco 1996; Metzger & Klewicki 2001) and DNS and PIV studies (Jimenez & del Alamo 2004; Christensen & Wu 2005; Ganapathisubramani *et al.* 2005). Furthermore, the inclusion of the detached eddy concept has been found to improve coherent motion-based model performance (Perry & Marusic 1995). Overall, layer III is nominally viewed as the region where the attached and detached eddies interact with highest probability.

(d) Characteristic dynamics

The properties of the MMB suggest that specific dynamical attributes may be associated with the attached/detached eddy structure proposed. For example, under the proposed model attached eddies form and evolve across layer II, and thus their dynamical signature is that they produce instantaneous contributions to positive $-\partial\bar{w}/\partial y$. Similarly, the characteristic eddies of layer IV are detached. Therefore, their dynamical signature is that they produce negative $-\partial\bar{w}/\partial y$. This identification of both a source and a sink character with the Reynolds stress term in the MMB is apparently distinct to the present model.

In the context of these dynamical signatures, it is useful to examine the equation

$$-\frac{\partial\bar{w}}{\partial y} = \overline{v\omega_z} - \overline{w\omega_y} + \frac{\partial}{\partial x} \left(\overline{v^2} + \overline{w^2} - \overline{u^2} \right). \quad (3.2)$$

For turbulent channel flow, the last term is identically zero, while for boundary layers this term is generally small.⁴ To a good approximation, however, the gradient of the Reynolds stress is largely established by the difference of the

⁴Hinze (1975) associated the vortical terms with Townsend's active motions and the streamwise derivative terms with the inactive motions.

indicated velocity vorticity correlations. Given this, the interpretation is that in layer II the attached eddies interact with the velocity field to generate a net positive sum, and in layer IV, the detached eddies generate a net negative sum. The dominant terms in equation (3.1) indicate that the dynamics underlying the evolution of attached eddies is characterized by a competition between viscous shear forces and turbulent inertia. During this evolution, these motions act as a source to the mean momentum, and at each Reynolds number this source-like character is, on an average, depleted at y_{\max} , the position of the peak in the Reynolds stress, T_{\max} . Similarly, detached eddy dynamics in layer IV is characterized by a competition between mean advection and turbulent inertia. On average, this sink-like character extends from y_{\max} to δ . The flow field interactions underlying equation (3.2) in either layer II or IV have been shown to have significant contributions from intermediate scale motions (Priyadarshana & Klewicki 2003). Physically, it is rational to attribute this to the fact that as $\delta^+ \rightarrow \infty$ velocity spectra peak at decreasingly low wavenumber, while vorticity spectra peak at increasingly high wavenumber. Thus, according to equation (3.2), the velocity and vorticity fields must correlate over some intermediate wavenumber range in order for there to be a net momentum transport via turbulent inertia. This argument, however, apparently only partially holds. Measurements over a very broad range of δ^+ indicate that with increasing δ^+ a spectrally local scale selection occurs. This results in significant contributions to the long-time correlation to arise from portions of the cospectra near the peaks in the participating velocity and vorticity spectra, respectively (Priyadarshana *et al.* 2007).

(e) *Inner/outer interactions*

The MMB-based model supports a clear set of perspectives regarding inner/outer interactions, some of which are now briefly discussed. One interpretation of the layer I–IV velocity increments is that the net circulation associated with the outward transport of vorticity from layer II (supporting boundary layer growth) is asymptotically balanced by a net inward transport of momentum from layer IV (required for the generation of a surface drag force; figure 4 and table 2). These attributes rather naturally align with the momentum source/sink character ascribed to the attached and detached eddies, respectively. Specifically, the attached and detached eddies are viewed as the active vortical mechanisms by which layer II turbulence is sustained (and near-wall vorticity is transported outward to layer IV), and by which free-stream momentum is extracted and transported into layer II, respectively. These physical attributes find consistency with perturbed boundary layer studies, indicating that the inner region rapidly adjusts, and following perturbation, rapidly recovers (e.g. Smits & Wood 1985). Conversely, recovery of the outer layer requires very long redevelopment lengths downstream of a perturbation (e.g. Eaton & Johnston 1981).

Another important feature is that the statistical centre of the inner/outer interaction is in layer III. This centres the interaction on the zone where the MMB undergoes a balance breaking and exchange; the net result being that the dynamics change from a balance between the viscous force and the turbulent inertia to a balance between the turbulent inertia and the mean advection. Similarly, the present model also attaches dynamical importance to the interaction between the motions that produce positive $-\partial\overline{w}/\partial y$ in layer II and those that produce negative $-\partial\overline{w}/\partial y$

in layer IV.⁵ In connection with this, increasing scale separation requires the aforementioned dynamical accommodation with increasing δ^+ , and thus the present model identifies an intermediate range of scales that continually adjusts with δ^+ as playing an essential role in the inner/outer interaction.

(f) *The logarithmic layer*

As noted in §2b, the prevalent model has rather direct connections to the mean profile and its overlap layer-based derivation of the logarithmic profile. Conversely, multiscale analyses of the MMB (for channel and Couette flow) reveal that a logarithmic profile is possible, but not by assuming the existence of an overlap layer. Specifically, through the use of an adjusted Reynolds stress function, Fife *et al.* (2005a,b) reveal that the MMB admits a scaling layer hierarchy that naturally gives rise to a length-scale distribution, and that these characteristic lengths asymptotically scale with y . Thus, these analyses provide a justification, rigorously founded in the MMB, for the distance from the wall scaling-based derivation of the logarithmic profile. They also identify the conditions required for the MMB to admit an exact logarithmic mean profile. Briefly, for each member of the family of adjusted Reynolds stresses (associated with the value of a parameter β), there corresponds a layer III-like structure across which the MMB undergoes a balance breaking and exchange. The length-scales associated with each of these layers can be rigorously derived according to the condition that when they are used to normalize the MMB, the MMB attains an invariant form. It follows that an exactly logarithmic mean profile will occur when the locally normalized second derivative of the Reynolds stress (divergence of the Lamb vector) remains invariant over a range of y (i.e. for a range of β). The layer hierarchy initiates near $y^+ = 30$ and terminates at $y/\delta \approx 0.5$ (Fife *et al.* 2005a). From this analysis, it is surmised that purely logarithmic behaviour is expected only over a range of y interior to these bounds, i.e. where ‘end effects’ do not disrupt the self-similarity of adjacent β layers. In general, however, the scale hierarchy covers part of layer II, all of layer III and part of layer IV. Interestingly, as noted in Wei *et al.* (2005a), this coverage of differing momentum balance layers provides a natural explanation for the existence and the observed break points of the varying logarithmic-like profile behaviours noted in §2. It is also worth mentioning the similarities between this mathematical structure and the findings regarding the hierarchical motion properties of the logarithmic layer. Among these is the potential correspondence between a given β layer and the statistical ensemble of hairpin vortex packets that rise to a given y -location.

4. Summary

A physical model of the turbulent boundary layer that is based upon the properties of the MMB has been described and compared with the prevalent, well-established, model. Some distinctions between the perspectives provided by the two models are

⁵Interestingly, support for particularly intense vortical motion interactions at intermediate scale is given by the remarkable observation that as δ^+ varies the peak in the dissipation spectra exhibits the same Reynolds number dependence as does the width of layer III (Tsuji 1999).

now briefly noted. In the prevalent model, the region where the effects of viscosity are deemed significant shrinks like $1/\delta^+$ with increasing δ^+ . In the present model, the region where the effects of viscosity are significant shrinks like $1/\sqrt{\delta^+}$. For the reasons discussed in §1, the implications of this difference are far reaching. The prevalent model derives perspectives relative to the Reynolds stress as a source of turbulent momentum transport. The present model derives perspectives from the source/sink properties of the Reynolds stress gradient relative to affecting a time rate of change of momentum. Distinct from the prevalent model, the present model centres the inner/outer interaction in the traditional logarithmic layer and in the region where the mean viscous force transitions to having a higher-order contribution to the dynamics. The prevalent model is most often discussed in connection with the assumption of an overlap layer and the corresponding derivation of the logarithmic mean profile. The present model incorporates the scale hierarchy-based derivation admitted by the MMB.

Lastly, some similarities and differences between the scale hierarchy and the overlap layer are worth noting. One similarity is that they constitute an internal intermediate layer, insulated from boundary condition effects, that exhibits self-similar behaviours according to local dynamics. The notion that a logarithmic layer is an inertial sublayer, however, requires clarification. The scale hierarchy exists in layers II, III and IV. According to the MMB, II and III are layers where the mean viscous and Reynolds stress gradients have the same order of magnitude. Thus, of these layers, only IV can rationally be considered an inertial layer. Interestingly, recent empirical results relating to where the ‘true’ logarithmic layer starts are consistent with this notion (see [Wei *et al.* 2005a](#)). Lastly, although it is not readily apparent how the overlap layer and the scale hierarchy descriptions might be equivalent, the possibility remains that both are valid descriptions of the same physics.

This work was supported by the National Science Foundation under grant CTS-0555223 and the Department of Energy under grant W-7405-ENG-48.

References

- Adrian, R. J., Meinhart, C. D. & Tomkins, C. D. 2000 Vortex organization in the outer region of the turbulent boundary layer. *J. Fluid Mech.* **422**, 1–54. (doi:10.1017/S0022112000001580)
- Bake, S., Meyer, D. G. W. & Rist, U. 2002 Turbulence mechanism in Klebanoff transition: a quantitative comparison of experiment and direct numerical simulation. *J. Fluid Mech.* **459**, 217–243. (doi:10.1017/S0022112002007954)
- Balint, J., Wallace, J. & Vukoslavcevic, P. 1991 The velocity and vorticity vector fields of a turbulent boundary layer. Part 2. Statistical properties. *J. Fluid Mech.* **228**, 53–86.
- Christensen, K. T. & Wu, Y. 2005 Characteristics of vortex organization in the outer layer of wall turbulence. In *Proc. Fourth Int. Symp. on Turbulence and Shear Flow Phenomena, Williamsburg, VA*, pp. 1025–1030.
- Davidson, P. 2004 *Turbulence: an introduction for scientists and engineers*. New York, NY: Oxford University Press.
- Davidson, P. A., Nickels, T. B. & Krogstad, P.-A. 2006 The logarithmic structure function law in wall-layer turbulence. *J. Fluid Mech.* **550**, 51–60. (doi:10.1017/S0022112005008001)
- DeGraaff, D. B. & Eaton, J. K. 2000 Reynolds number scaling of the flat plate turbulent boundary layer. *J. Fluid Mech.* **422**, 319–346. (doi:10.1017/S0022112000001713)
- Eaton, J. K. & Johnston, J. P. 1981 A review of research on subsonic flow reattachment. *AIAA J.* **19**, 1093–1102.

- Falco, R. E. 1977 Coherent motions in the outer region of turbulent boundary layers. *Phys. Fluids* **20**, S124–S132. (doi:10.1063/1.861721)
- Falco, R. E. 1983 New results, a review and synthesis of the mechanism of turbulence production in boundary layers and its modification. AIAA paper no. 83-0377.
- Falco, R. E. 1991 A coherent structure model of the turbulent boundary layer and its ability to predict Reynolds number dependence. *Phil. Trans R. Soc. A* **336**, 103–129.
- Fife, P., Wei, T., Klewicki, J. & McMurtry, P. 2005a Stress gradient balance layers and scale hierarchies in wall bounded turbulent flows. *J. Fluid Mech.* **532**, 165–189. (doi:10.1017/S0022112005003988)
- Fife, P., Klewicki, J., McMurtry, P. & Wei, T. 2005b Multiscaling in the presence of indeterminacy: wall-induced turbulence. *Multiscale Model. Simul.* **4**, 936–959. (doi:10.1137/040611173)
- Ganapathisubramani, B., Longmire, E. K. & Marusic, I. 2003 Characteristics of vortex packets in turbulent boundary layers. *J. Fluid Mech.* **478**, 35–46. (doi:10.1017/S0022112002003270)
- Ganapathisubramani, B., Hutchins, N., Hambleton, W. T., Longmire, E. K. & Marusic, I. 2005 Investigation of large-scale coherence in a turbulent boundary layer using two-point correlations. *J. Fluid Mech.* **524**, 57–80. (doi:10.1017/S0022112004002277)
- Head, M. R. & Bandyopadhyay, P. 1981 New aspects of turbulent boundary layer structure. *J. Fluid Mech.* **107**, 297–338. (doi:10.1017/S0022112081001791)
- Hinze, J. O. 1975 *Turbulence*. New York, NY: McGraw-Hill.
- Jimenez, J. & del Alamo, J. C. 2004 Computing turbulent channels at experimental Reynolds numbers. In *Proc. 15th Australasian Fluid Mechanics Conference, The University of Sydney, Australia*, paper no. AFMC00038.
- Kim, J., Moin, P. & Moser, R. 1987 Turbulence statistics in fully-developed channel flow at low Reynolds number. *J. Fluid Mech.* **177**, 133–166. (doi:10.1017/S0022112087000892)
- Klewicki, J. C. 1989 On the interactions between the inner and outer region motions in turbulent boundary layers. Ph.D. dissertation, Michigan State University.
- Klewicki, J. C. 1997 Self-sustaining traits of near-wall motions underlying boundary layer stress transport. In *Self-sustaining mechanisms of wall turbulence* (ed. R. L. Panton), pp. 135–166. Southampton, UK: Computational Mechanics Publications.
- Klewicki, J. C. & Falco, R. E. 1990 On accurately measuring statistics associated with small-scale structure in turbulent boundary layers using hot-wire probes. *J. Fluid Mech.* **219**, 119–142. (doi:10.1017/S0022112090002889)
- Klewicki, J. C. & Falco, R. E. 1996 Spanwise vorticity structure in turbulent boundary layers. *Int. J. Heat Fluid Flow* **17**, 363–376. (doi:10.1016/0142-727X(96)80001-W)
- Klewicki, J. C., Gendrich, C. P., Foss, J. F. & Falco, R. E. 1990 On the sign of the instantaneous spanwise vorticity component in the near-wall region of turbulent boundary layers. *Phys. Fluids A* **2**, 1497–1500. (doi:10.1063/1.857599)
- Kline, S. J. 1978 The role of visualization in the study of the structure of the turbulent. In *Coherent structure of turbulent boundary layers, an AFOSR/Lehigh University Workshop* (eds C. R. Smith & D. E. Abbott), p. 1. Bethlehem, PA: Lehigh University.
- McKeon, B. & Morrison, J. 2007 Asymptotic scaling in turbulent pipe flow. *Proc. R. Soc. A* **365**, 771–787. (doi:10.1098/rsta.2006.1945)
- McKeon, B., Li, J., Jiang, W., Morrison, J. & Smits, A. 2004 Further observations on the velocity distribution in fully-developed pipe flow. *J. Fluid Mech.* **501**, 135–147. (doi:10.1017/S0022112003007304)
- Meinhart, C. & Adrian, R. 1995 On the existence of uniform momentum zones in a turbulent boundary layer. *Phys. Fluids* **7**, 694–696. (doi:10.1063/1.868594)
- Metzger, M. M. 2006 Length scales and time scales of the near-surface axial velocity in a high Reynolds number turbulent boundary layer. *Int. J. Heat Fluid Flow* **27**, 534–541.
- Metzger, M. M. & Klewicki, J. C. 2001 A comparative study of wall region structure in high and low Reynolds number turbulent boundary layers. *Phys. Fluids* **13**, 692–701. (doi:10.1063/1.1344894)

- Millikan, C. 1939 A critical discussion of turbulent flows in channels and circular tubes. In *Proc. Fifth Int. Congress of Applied Mechanics*, pp. 5772–5776. New York, NY: Wiley.
- Moin, P., Leonard, A. & Kim, J. 1986 Evolution of a curved vortex filament into a vortex ring. *Phys. Fluids* **29**, 955–963. (doi:10.1063/1.865690)
- Morris, S., Stolpa, S., Slaboch, P. & Klewicki, J. In press. Near surface particle image velocimetry measurements in a transitionally rough-wall atmospheric boundary layer. *J. Fluid Mech.*
- Morrison, J., McKeon, B., Jiang, W. & Smits, A. 2004 Scaling of the streamwise velocity component in turbulent pipe flow. *J. Fluid Mech.* **508**, 99–131. (doi:10.1017/S0022112004008985)
- Moser, R. D., Kim, J. & Mansour, N. N. 1999 Direct numerical simulation of turbulent channel flow up to $R_\tau=590$. *Phys. Fluids* **11**, 943–945. (doi:10.1063/1.869966)
- Offen, G. R. & Kline, S. J. 1974 Combined dye streak and Hydrogen-bubble visual observations of a turbulent boundary layer. *J. Fluid Mech.* **62**, 223–239. (doi:10.1017/S0022112074000656)
- Osterlund, J., Johansson, A., Nagib, H. & Hites, M. 2000 A note on the overlap region in turbulent boundary layers. *Phys. Fluids* **12**, 1–4. (doi:10.1063/1.870250)
- Panton, R. L. 1997 *Self-sustaining mechanisms of wall turbulence*. Southampton, UK: Computational Mechanics Publications.
- Panton, R. L. 2005 Review of wall turbulence as described by composite expansions. *Appl. Mech. Rev.* **58**, 1–36. (doi:10.1115/1.1840903)
- Perry, A. E. & Abell, C. J. 1977 Asymptotic similarity of turbulence structures in smooth- and rough-wall pipes. *J. Fluid Mech.* **79**, 785–799. (doi:10.1017/S0022112077000457)
- Perry, A. E. & Chong, M. S. 1982 On the mechanism of wall turbulence. *J. Fluid Mech.* **119**, 173–217. (doi:10.1017/S0022112082001311)
- Perry, A. E. & Marusic, I. 1995 A wall-wake model for the turbulence structure of boundary layers. Part 1. Extensions of the attached eddy hypothesis. *J. Fluid Mech.* **298**, 361–388. (doi:10.1017/S0022112095003351)
- Perry, A. E., Henbest, S. & Chong, M. S. 1986 A theoretical and experimental study of wall turbulence. *J. Fluid Mech.* **165**, 163–199. (doi:10.1017/S002211208600304X)
- Pope, S. B. 2000 *Turbulent flow*. Cambridge, UK: Cambridge University Press.
- Prandtl, L. 1904 Über flüssigkeitsbewegungen bei sehr kleiner reibung. In *Verhandlungen des Dritten Internationalen Mathematiker-Kongresses in Heidelberg 1904* (ed. A. Krazer), pp. 484–491. Leipzig, Germany: Teubner.
- Prandtl, L. 1925 Bericht über die Entstehung der Turbulenz. *Z. Agnew. Math. Mech.* **5**, 136–139.
- Priyadarshana, P. & Klewicki, J. C. 2003 Reynolds number scaling of wall layer velocity–vorticity products. In *Reynolds number scaling in turbulent flow* (ed. A. J. Smits), pp. 117–122. Princeton, NJ: Kluwer Academic Publishers.
- Priyadarshana, P., Klewicki, J., Treat, S. & Foss, J. 2007 Statistical structure of turbulent boundary layer velocity–vorticity products at high and low Reynolds numbers. *J. Fluid Mech.* **570**, 307–346. (doi:10.1017/S0022112006002771)
- Rajagopalan, S. & Antonia, R. A. 1993 Structure of the velocity field associated with the spanwise vorticity in the wall region of a turbulent boundary layer. *Phys. Fluids A* **5**, 2502–2510. (doi:10.1063/1.858763)
- Robinson, S. K. 1990 Coherent motions in the turbulent boundary layer. *Annu. Rev. Fluid Mech.* **23**, 601–639. (doi:10.1146/annurev.fl.23.010191.003125)
- Schlichting, H. 1979 *Boundary layer theory*. New York, NY: McGraw-Hill.
- Smith, C. R., Walker, J. D. A., Haidari, A. H. & Sobrun, U. 1991 On the dynamics of near-wall turbulence. *Phil. Trans. R. Soc. A* **336**, 131–175.
- Smits, A. J. & Wood, D. H. 1985 The response of turbulent boundary layers to sudden perturbations. *Annu. Rev. Fluid Mech.* **17**, 321–358. (doi:10.1146/annurev.fl.17.010185.001541)
- Spalart, P. 1988 Direct simulation of a turbulent boundary layer up to $R_\theta=1410$. *J. Fluid Mech.* **187**, 61–98. (doi:10.1017/S0022112088000345)
- Sreenivasan, K. R. 1989 The turbulent boundary layer. In *Frontiers in experimental fluid mechanics*, vol. 46 (ed. M. Gad-el-Hak). Springer Lecture Notes in Engineering, pp. 159–209. Berlin, Germany: Springer.

- Tennekes, H. & Lumley, J. 1972 *A first course in turbulence*. Cambridge, MA: MIT Press.
- Theodorsen, T. 1952 Mechanism of turbulence. In *Proc. 2nd Midwestern Conf. on Fluid Mechanics*, pp. 1–19. Columbus, OH: The Ohio State University.
- Thomas, A. S. W. & Bull, M. K. 1983 On the role of pressure fluctuations in deterministic motions in the turbulent boundary layer. *J. Fluid Mech.* **128**, 283–322. (doi:10.1017/S002211208300049X)
- Tomkins, C. D. & Adrian, R. J. 2003 Spanwise structure and scale growth in turbulent boundary layers. *J. Fluid Mech.* **490**, 37–74. (doi:10.1017/S0022112003005251)
- Townsend, A. A. 1976 *The structure of turbulent shear flow*. Cambridge, UK: Cambridge University Press.
- Tsuji, Y. 1999 Peak position of dissipation spectrum in turbulent boundary layers. *Phys. Rev. E* **59**, 7235–7238. (doi:10.1103/PhysRevE.59.7235)
- Wallace, J. M. 1982 On the structure of turbulent shear flow. A personal view. In *Developments in theoretical and applied mechanics* (eds T. J. Chung & G. Karr), pp. 1–12. Huntsville, AL: Department of Mechanical Engineering, University of Alabama.
- Wark, C. E. & Nagib, H. M. 1991 Experimental investigation of coherent structures on turbulent boundary layers. *J. Fluid Mech.* **230**, 183–208. (doi:10.1017/S0022112091000757)
- Wei, T., Fife, P., Klewicki, J. & McMurtry, P. 2005a Properties of the mean momentum balance in turbulent boundary layer, pipe and channel flows. *J. Fluid Mech.* **522**, 303–327. (doi:10.1017/S0022112004001958)
- Wei, T., McMurtry, P., Klewicki, J. & Fife, P. 2005b Meso scaling of the Reynolds shear stress in turbulent channel and pipe flows. *AIAA J.* **43**, 2350–2353.
- Wosnik, M., Castillo, L. & George, W. K. 2000 A theory for turbulent pipe and channel flows. *J. Fluid Mech.* **421**, 115–145. (doi:10.1017/S0022112000001385)
- Zagarola, M. V. & Smits, A. J. 1997 Scaling of the mean velocity profile for turbulent pipe flow. *Phys. Rev. Lett.* **78**, 239–242. (doi:10.1103/PhysRevLett.78.239)